

## Actively Contracting Bundles of Polar Filaments

K. Kruse<sup>1,2</sup> and F. Jülicher<sup>1</sup>

<sup>1</sup>*Institut Curie, Physicochimie, UMR CNRS/IC 168, 26 rue d'Ulm, 75248 Paris Cedex 05, France*

<sup>2</sup>*Max-Planck-Institut für Strömungsforschung, Bunsenstrasse 10, D-37073 Göttingen, Germany*

(Received 3 April 2000)

We introduce a phenomenological model to study the properties of bundles of polar filaments which interact via active elements. The stability of the homogeneous state, the attractors of the dynamics in the unstable regime, and the tensile stress generated in the bundle are discussed. We find that the interaction of parallel filaments can induce unstable behavior and is responsible for active contraction and tension in the bundle. The interaction between antiparallel filaments leads to filament sorting. Our model could apply to simple contractile structures in cells such as stress fibers.

PACS numbers: 87.16.Ka, 05.45.Ac, 47.54.+r, 87.15.La

Living cells have remarkable mechanical properties. In addition to a passive response to mechanical stresses, eucaryotic cells are able to actively change their shapes, to generate motion and forces [1], and to react to externally imposed mechanical conditions [2]. The cytoskeleton, which is a complex network of elastic protein filaments such as actin filaments and microtubules, plays a key role in these processes. Filaments are rod-like structures that interact with a large number of specific proteins [3]. Examples are cross-linking proteins which induce formation of a gel-like filament network and bundling proteins which lead to filaments aligned in parallel. Furthermore, motor proteins of the cytoskeleton are able to use the chemical energy of the hydrolysis of adenosinetriphosphate (ATP) to generate forces and motion along the filaments [1,3–5]. Myosins, for example, interact with actin filaments while kinesins and dyneins move along microtubules. The direction of motion of motor molecules is determined by the polar structure of the filaments which have two different ends, one denoted “plus,” the other “minus”: a given type of motors always moves towards the same end [1]. Small aggregates of motors which contain two or more active domains can bind at the same time to two filaments and exert relative forces and motion between them. In contrast to passive filament solutions whose rheological properties have been studied in recent years [6], filament systems which interact with molecular motors represent intrinsically active materials which exhibit rich types of behavior that have recently attracted much interest. In particular, the formation of asters and spiral defects as well as the shortening of filament bundles have been observed *in vitro* and *in vivo* [7–10]. The self-organization of motor-filament systems has also been addressed theoretically [11–13].

Bundles of actin filaments interacting with myosin motors are prominent cytoskeletal structures that are involved in many active phenomena in the cell [1]. For example, within the sarcomeres of skeletal muscle fibers, they are responsible for muscle contraction; as stress fibers they produce forces in cells; and as contractile rings they are important during the final step of cell division. The contraction of sarcomeres follows from a particular arrangement

of myosin and actin filaments. In contrast, stress fibers and related structures lack an obvious spatial organization of their components. The existence of these simple contractile structures raises interesting questions: What are the minimal requirements for a bundle of filaments and active elements to contract? Do stable steady states of the bundle exist which generate tension?

In this Letter, we develop a simple phenomenological model for bundles of polar filaments containing active elements that allows us to answer such questions and to estimate the mechanical tension generated in the bundle. Furthermore, we perform computer simulations which demonstrate that the general behaviors described by this model are indeed obtained for simple realizations of the motor-filament interactions. Finally, we relate our findings to biological systems.

Consider a linear bundle of aligned polar filaments of equal length  $\ell$  distributed along the  $x$  axis. The number densities of filaments with their plus ends pointing to the right and to the left and with their center located at position  $x$  are denoted  $c^+(x)$  and  $c^-(x)$ , respectively. These densities satisfy the conservation laws

$$\begin{aligned}\partial_t c^+ &= D \partial_x^2 c^+ - \partial_x J^{++} - \partial_x J^{+-}, \\ \partial_t c^- &= D \partial_x^2 c^- - \partial_x J^{-+} - \partial_x J^{--}.\end{aligned}\quad (1)$$

Here,  $D$  is an effective coefficient for filament diffusion along the  $x$  axis. The currents  $J^{+-}$  and  $J^{-+}$  are active filament currents that result from interactions mediated by motors between pairs of antiparallel filaments. Currents resulting from interactions between parallel filaments are denoted  $J^{++}$  and  $J^{--}$ . Here, we have assumed for simplicity that two-filament interactions dominate, which corresponds to a sufficiently low density of active elements. Equation (1) thus corresponds to a coarse-grained description where details of the dynamics of the motors have been eliminated. The direction of filament motion induced by a motor depends only on the filaments' relative orientation; see Fig. 1. Therefore, we can use general symmetry arguments to write expressions for the active currents without referring to a specific interaction mechanism.

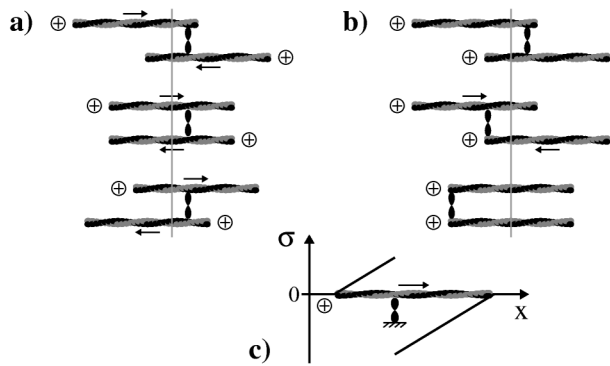


FIG. 1. Schematic representation of motor-filament interactions. Motors are assumed to move towards the plus end of filaments; arrows indicate the direction of filament motion. Vertical lines indicate the centers of gravity of the filament pair. (a) Antiparallel filaments slide in opposite directions. (b) Relative motion of parallel filaments occurs if a motor binds to a plus end. Parallel filaments thus have the tendency to align their plus ends. (c) Tension profile  $\sigma$  along a filament driven by a point force.

To this end we express the currents in terms of the filament densities  $c^+$  and  $c^-$ . For example, we write  $J^{+-}(x) = \int_{-\ell}^{\ell} d\xi j^{+-}(x, \xi)$ , where  $j^{+-}(x, \xi)$  is the average current of plus filaments located at  $x$  induced by the interaction with minus filaments located at  $x + \xi$ . The integral arises since all filaments with centers located in the interval  $[x - \ell, x + \ell]$  can interact with a filament located at  $x$ . Then, assuming that the probability for an active interaction between two filaments depends only on the probability of their encounter, we write  $j^{+-}(x, \xi) = v^{+-}(\xi)c^+(x)c^-(x + \xi)$ . Here,  $v^{+-}(\xi)$  is the effective relative velocity between two antiparallel filaments a distance  $\xi$  apart induced by many individual events of motor activity. For parallel filaments we get analogously, e.g.,  $j^{++} = v^{++}(\xi)c^+(x)c^+(x + \xi)$ . Now, symmetry arguments restrict the possible form of the functions  $v^{\pm\pm}$  and  $v^{\pm\mp}$ : In the absence of external forces momentum conservation requires that the center of gravity must remain fixed when two filaments are displaced. This leads to  $v^{\pm\pm}(\xi) = -v^{\pm\pm}(-\xi)$  and  $v^{+-}(\xi) = -v^{+-}(-\xi)$ ; see Fig. 1. Furthermore, invariance of the system with respect to inversions of space leads to the condition  $v^{++}(\xi) = -v^{--}(-\xi)$ . Respecting these criteria, we choose for simplicity  $v^{+-}(\xi) = -v^{+-}(\xi) = \beta$  and  $v^{++}(\xi) = v^{--}(\xi) = \alpha \text{sign}(\xi)$ . Here,  $\alpha$  and  $\beta$  are constants and  $\text{sign}(\xi) = \pm 1$ , depending on the sign of  $\xi$ . We have checked that other choices do not alter the general properties of our model. The currents thus read

$$J^{++}(x) = \alpha \int_0^{\ell} d\xi [c^+(x + \xi) - c^+(x - \xi)]c^+(x), \quad (2)$$

$$J^{+-}(x) = \mp \beta \int_{-\ell}^{\ell} d\xi c^{\mp}(x + \xi)c^{\pm}(x).$$

Equations (1) and (2) describe the dynamics of our model. We first analyze the stability of the homogeneous state

with constant  $c^{\pm}(x) = c_0^{\pm}$ , which is a fixed point of the dynamics for all values of the parameters. Using a Fourier expansion of the densities  $c^{\pm}(x) = c_0^{\pm} + \sum_k c_k^{\pm} e^{ikx}$ , the filament dynamics to linear order in the amplitudes  $c_k^{\pm}$  is given by

$$\frac{d}{dt} \begin{pmatrix} c_k^+ \\ c_k^- \end{pmatrix} = \begin{pmatrix} \Lambda^{++} & \Lambda^{+-} \\ \Lambda^{-+} & \Lambda^{--} \end{pmatrix} \begin{pmatrix} c_k^+ \\ c_k^- \end{pmatrix}, \quad (3)$$

where the elements of the matrix  $\Lambda(k)$  are

$$\Lambda^{\pm\pm}(k) = -Dk^2 - 2\alpha[\cos(k\ell) - 1]c_0^{\pm} \pm 2i\beta k\ell c_0^{\mp},$$

$$\Lambda^{\pm\mp}(k) = \pm 2i\beta \sin(k\ell)c_0^{\pm}. \quad (4)$$

With  $\lambda(k)$  denoting the larger of the real parts of the two eigenvalues of the matrix  $\Lambda(k)$ , the homogeneous state is stable if  $\lambda(k) \leq 0$  for all  $k$ . When an instability occurs, a band of unstable modes appears, which extends from  $k = 0$  to some positive  $k$ . For a system of size  $L$  with periodic boundary conditions (e.g., a contractile ring), the stability of the homogeneous state is determined by the sign of  $\lambda(k_{\min})$ , with  $k_{\min} = 2\pi/L$ . We find that the homogeneous state becomes linearly unstable as soon as  $\alpha > \alpha_c$  with the critical value

$$\alpha_c = \frac{D}{\ell^2 c} f\left(\frac{\beta\ell cL}{D}, \frac{\delta c}{c}, \frac{L}{\ell}\right). \quad (5)$$

Here  $c \equiv c_0^+ + c_0^-$ ,  $\delta c \equiv c_0^+ - c_0^-$ , and  $f(u, v, w)$  is a dimensionless scaling function. Corresponding stability diagrams are displayed in Fig. 2. For all values of the parameters we find  $\alpha_c \geq 0$ . Therefore, unstable behavior is induced by an interaction of parallel filaments with  $\alpha > 0$ . Consistent with this finding  $\alpha_c$  decreases with increasing  $\delta c$ , i.e., with an increasing fraction of filaments pointing in the same direction the system becomes less stable. The

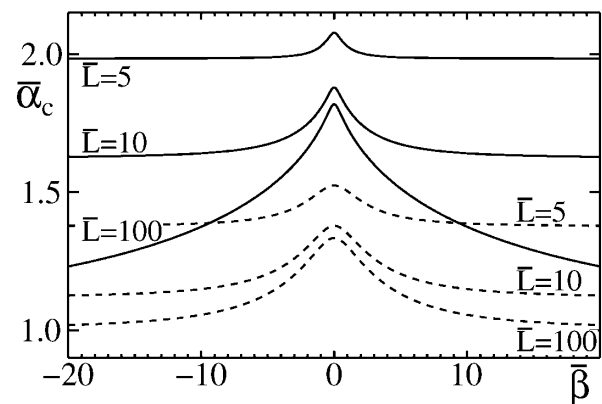


FIG. 2. The critical value  $\bar{\alpha}_c = \alpha_c \ell^2 c / D$  as a function of  $\bar{\beta} = \beta \ell c L / D$  for different values of  $\bar{L} = L / \ell$ . Here,  $\alpha$  and  $\beta$  characterize the interaction strength of parallel and antiparallel filaments, respectively,  $L$  is the system size and  $\ell$  the filament length. Solid lines correspond to  $\delta c = c/10$  and dashed lines to  $\delta c = c/2$ , where  $c$  is the filament density and  $\delta c/c$  the relative difference of the densities of plus and minus filaments. The homogeneous state is unstable for  $\alpha > \alpha_c$ .

critical value  $\alpha_c$  increases with increasing  $D$ , indicating that filament diffusion has a stabilizing effect. In many limiting cases simple analytic expressions for  $\alpha_c$  can be obtained. In particular, we find in the limit of large  $L$ ,  $f = 2/(1 + |\delta c|/c)$  if  $\beta = 0$  or  $\delta c = 0$  and  $f = 1$  otherwise. In the homogeneous state, the total filament current  $J = J^{++} + J^{+-} + J^{-+} + J^{--}$  vanishes, while currents of plus and minus filaments exist in opposite directions. As soon as the homogeneous state becomes unstable, a transient current  $J$  occurs which redistributes filaments until an inhomogeneous stationary state is attained. This final state consists of one or several shortened filament bundles separated by empty regions. Figure 3 displays the variance  $\langle x^2 \rangle = \int dx x^2 (c^+ + c^-)$  of stationary filament distributions as a function of  $\alpha$ , where we have assumed without loss of generality that  $\int dx x (c^+ + c^-) = 0$ . For small  $\alpha$  only the homogeneous state exists as the attractor of the system. A second attractor appears for  $\alpha = \alpha_d < \alpha_c$ , which corresponds to a shortened filament bundle. A third type of attractor obtained numerically consists of two shortened filament bundles. However, we cannot distinguish numerically whether this state is a real attractor or a long-lived transient state.

The instability of the homogeneous state thus leads to bundle shortening. It is triggered by an increase of  $\alpha$  and occurs for all values of  $\beta$ , which suggests that the interaction of parallel filaments is responsible for bundle shortening. On the other hand, the interaction of anti-parallel filaments ( $\beta \neq 0$ ) induces currents which in the unstable regime lead to a separation of plus and minus filaments [11]. The role of interactions between parallel filaments for bundle shortening can be demonstrated explicitly for the simple case  $D = 0$  for which the uniform state is linearly unstable for all  $\alpha > 0$ . In this case, using Eqs. (1) and (2), we can show that for  $\beta = 0$  and  $\alpha > 0$  the vari-

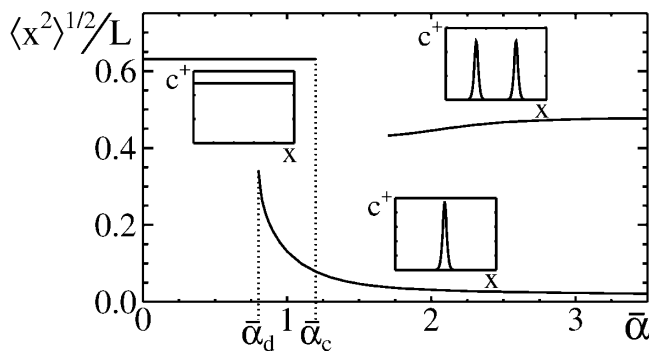


FIG. 3. Variance of stable stationary filament distributions as a function of  $\bar{\alpha} = \alpha \ell^2 c / D$  obtained by numerical solution of Eqs. (1) and (2) for  $L = 10\ell$  and a system containing plus filaments only ( $c^- = 0$ ). The homogeneous state is stable for  $\bar{\alpha} < \bar{\alpha}_c$ . For  $\bar{\alpha} > \bar{\alpha}_d$  a new attractor corresponding to a shortened bundle appears. A third attractor is also indicated. The insets show for each attractor typical filament distributions over one period in arbitrary units.

ance decreases monotonically, i.e.,  $d/dt \langle x^2 \rangle < 0$ , which implies bundle shortening.

Can the active filament interactions which lead to bundle shortening generate tensile stresses that can be used to perform mechanical work during shortening? In the bundle, tension arises due to forces generated by motors and due to hydrodynamic forces exerted on the filaments by the surrounding fluid. Let us estimate this tension  $\sigma$  which has units of force. For simplicity, we take only local friction into account and ignore interactions between different filaments by friction forces. Consider a rigid rod-like filament moving in a viscous environment in the direction of its axis with a friction coefficient per unit length  $\eta$ . If this motion is induced by a locally applied force, then the tension profile along the filament is piecewise linear; see Fig. 1(c). Tension is positive in the rear part of the filament being “pulled” and negative in the front. Using this tension profile, we calculate an average tension profile along a filament at position  $x$  by summing over all contributions due to interactions with filaments lying in the interval  $[x - \ell, x + \ell]$ . We then calculate the tension in the bundle at position  $y$ , by summing the average tension of all filaments with centers within the interval  $[y - \ell/2, y + \ell/2]$ . Finally, we coarse grain over one filament length and obtain  $\sigma(y) = \sigma^{++}(y) + \sigma^{+-}(y) + \sigma^{-+}(y) + \sigma^{--}(y)$ , where

$$\begin{aligned} \sigma^{\pm\pm} &= \bar{\eta} \ell \alpha \int_{y-\ell/2}^{y+\ell/2} dx \int_{-l}^{\ell} d\xi c^{\pm}(x + \xi) c^{\pm}(x), \\ \sigma^{\pm\mp} &= \mp \bar{\eta} \ell \beta \int_{y-\ell/2}^{y+\ell/2} dx \int_0^{\ell} d\xi \\ &\quad \times [c^{\mp}(x + \xi) - c^{\mp}(x - \xi)] c^{\pm}(x). \end{aligned}$$

Here,  $\bar{\eta}$ ,  $\bar{\eta}$  are effective frictions per unit length which result from the coarse graining and differ from  $\eta$  by dimensionless geometric factors. Note, that the final coarse-grained tension profile is independent of microscopic details of the interaction mechanism.

As an example, consider a homogeneous ring, i.e., periodic boundary conditions. According to the above equation it generates a tension  $\sigma = 2\alpha \bar{\eta} \ell^3 (c_0^{+2} + c_0^{-2})$ , which for  $\alpha > 0$  is positive and could then lead to active contraction of the ring. This tension persists only if the homogeneous state is stable. As soon as an instability occurs, i.e., for  $\alpha > \alpha_c$ , the ring ruptures and the remaining bundle subsequently shortens. The shortening of the unstable bundle generates transient inhomogeneous tension profiles. Figure 4 displays instantaneous density and tension profiles of a filament bundle during shortening. The density profile is symmetric, vanishing at the bundle ends. The tension profile has the same qualitative shape. The inhomogeneous tension leads to a filament current  $J(x)$  which is antisymmetric corresponding to filament motion towards the bundle center, consistent with bundle shortening.

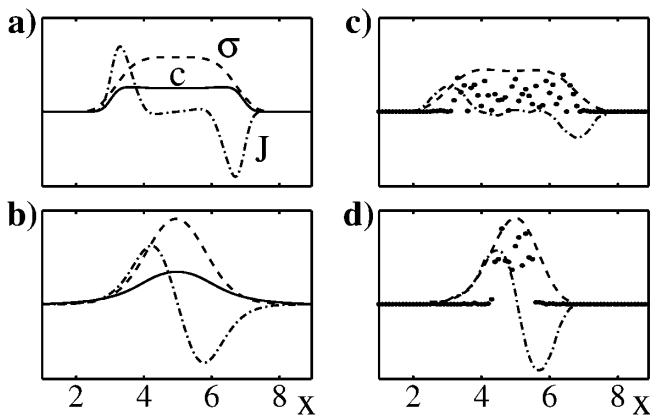


FIG. 4. Instantaneous filament distributions (full lines, dots), the tension profile (dashed lines), and the current (dash-dotted lines) in arbitrary units of contracting filament bundles. (a), (b) Numerical solutions of Eqs. (1) and (2) with  $\bar{\alpha} = 0.5$ ,  $\bar{\beta} = 0$ ,  $c = 0.5$ ,  $\delta c = 1$ , and  $\bar{L} = 10$ . (c), (d) Simulation of  $N = 1000$  filaments as described in the text. (a) and (c) are for earlier times, (b) and (d) for later times.

The effective model discussed above does not specify the microscopic origin of active filament interactions characterized by  $\alpha$  and  $\beta$ . In particular, the interaction between parallel filaments could seem surprising [14]. In order to demonstrate that such interactions can emerge naturally from simple motor-filament interactions we have performed computer simulations of a more microscopic model. We consider  $N$  rigid filaments aligned along the  $x$  axis. During each time step, a motor complex creates a mobile cross-link between a randomly chosen pair of filaments. The motors are displaced towards the plus ends of the filaments with velocity  $v$ , possibly leading to a relative filament displacement. This generates an interaction between antiparallel filaments. A relative displacement between parallel filaments occurs if we, furthermore, assume that the filament ends have different properties than the bulk of the filaments, namely, a motor which binds to or arrives at the plus end of a filament stays attached for some time; see Fig. 1(b). This effect generates an effective interaction with  $\alpha > 0$  between parallel filaments [15]. We have added diffusion steps in the simulations with  $D \neq 0$ . Our simulations show the same qualitative behaviors discussed above for the phenomenological model: an instability of the homogeneous state which occurs below a characteristic value of  $D$ . In the unstable state we observe bundle shortening due to the interaction of parallel filaments; interaction of anti-parallel filaments leads to a separation of plus and minus filaments. Using piecewise linear tension profiles for moving filaments (corresponding to local friction), we determine  $\sigma(x)$  in our simulation by averaging over many numerical steps. For the homogeneous state we find a tension which fluctuates around a constant positive value. The simulated density profile, tension profile, and averaged filament current of a shortening bundle are displayed in Fig. 4.

In conclusion, we have demonstrated that a bundle of aligned filaments and motors may contract and generate tension even if it is lacking a spatial organization. Using symmetry arguments, we have shown under some simplifying assumptions that the interaction of parallel filaments is important. Whether stress fibers in cells use the physical mechanism proposed here for contraction remains to be tested. In particular, experiments which focus on the interaction between parallel filaments should be performed. Stress fibers are likely to be more complex than the system studied here and might also use other mechanisms for contraction. For example, they could have some yet unknown spatial organization that allows them to contract more efficiently, or other components in addition to motors and filaments might be involved. Furthermore, they might work close to the percolation threshold where large filament aggregates occur and which is not captured by our model. Nevertheless, we think that our model helps clarify the role of motor-filament interactions and self-organization phenomena for force generation in biological cells.

We thank M. Bornens, S. Camalet, P. Janmey, A. Maggs, F. Nédélec, A. Ott, A. Parmeggiani, M. Piel, J. Prost, and A. B. Verkhovsky for stimulating discussions.

- 
- [1] B. Alberts *et al.*, *The Molecular Biology of the Cell* (Garland, New York, 1994), 3rd ed.
  - [2] O. Thoumine and A. Ott, *MRS Bull.* **24**, 22 (1999).
  - [3] T. Kreis and R. Vale, *Cytoskeletal and Motor Proteins* (Oxford University Press, New York, 1993).
  - [4] J. Howard, *Nature (London)* **389**, 561 (1997).
  - [5] F. Jülicher, A. Ajdari, and J. Prost, *Rev. Mod. Phys.* **69**, 1269 (1997).
  - [6] F. C. MacKintosh and P. A. Janmey, *Curr. Opin. Solid State Mater. Sci.* **2**, 350 (1997).
  - [7] K. Takiguchi, *J. Biochem. (Tokyo)* **109**, 502 (1991).
  - [8] A. B. Verkhovsky, T. M. Svitkina, and G. G. Borisy, *J. Cell Sci.* **110**, 1693 (1997).
  - [9] F. J. Nédélec *et al.*, *Nature (London)* **389**, 305 (1997).
  - [10] T. Surrey *et al.*, *Proc. Natl. Acad. Sci. U.S.A.* **95**, 4293 (1998).
  - [11] H. Nakazawa and K. Sekimoto, *J. Phys. Soc. Jpn.* **65**, 2404 (1996).
  - [12] K. Sekimoto and H. Nakazawa, in *Current Topics in Physics*, edited by Y. M. Cho, J. B. Hong, and C. N. Yang (World Scientific, Singapore, 1998), Vol. 1, p. 394; physics/0004044.
  - [13] B. Basetti, M. Cosentino Lagomarsino, and P. Jona, *cond-mat/9911140* (1999).
  - [14] There is however evidence for active interactions of parallel microtubules; see A. A. Hyman and E. Karsenti, *Cell* **84**, 401 (1996).
  - [15] In general, an interaction between parallel filaments is generated if motor function depends on the distance of the motor from the filament ends. Note, that the sign of  $\alpha$  depends on the details of the mechanism.